FEATURE ARTICLE

Journal of Materials Chemistry
www.rsc.org/materials

Metal encapsulated nanotubes of silicon and germanium

Abhishek Kumar Singh,*[a] Vijay Kumar[a,b] and Yoshiyuki Kawazoe[b]

[a]*Institute for Materials Research, Tohoku University, Aoba-ku, Sendai 980-8577, Japan. E-mail: abhishek@imr.edu; Fax: 81-22-215-2052; Tel: 81-22-215-2057*
[b]*Dr. Vijay Kumar Foundation, 45 Bazaar Street, K. K. Nagar (West), Chennai 600 078, India*

Received 25th September 2003, Accepted 10th December 2003
First published as an Advance Article on the web 22nd January 2004

Nanoforms of silicon such as nanoparticles and nanowires have been attracting much attention and recent findings of novel metal encapsulated silicon clusters as well as nanotubes have opened up new avenues for the development of silicon nanostructures. We review these recent developments and discuss the findings of the metal encapsulated nanotubes of silicon and germanium using *ab initio* total energy calculations. These nanotubes are generally found to be metallic. The metalicity is not induced by the doping of metal atoms, though they stabilize silicon and germanium in tubular forms. Transition metal atoms such as Mn and Fe lead to nanotubes that are ferromagnetic making them interesting as nanomagnets. Antiferromagnetic and ferrimagnetic phases have also been obtained. A novel aspect of these magnetic nanotubes is the possibility of developing half-metallic nanotubes that could be interesting for nano-spintronics applications. Further possibilities of semiconducting silicon nanotubes are discussed.

Introduction

Quasi-one-dimensional nanostructures such as nanotubes and nanowires are currently of great interest due to the possibilities for their applications in miniature devices. Therefore, much effort is being devoted to develop a fundamental understanding of the electrical, optical, magnetic, and mechanical properties of such materials and their dependence on size as well as interaction with other species. Extensive research on carbon nanotubes[1] over the past decade has shown a wide range of possible applications. Carbon nanotubes can be metallic or

Abhishek Kumar Singh did his M.Sc. in Physics at the Indian institute of Technology, Delhi, India. He is currently a MEXT fellow carrying out his Ph.D. in computational materials science at the Tohoku University, Sendai. He was the Vice President of the Physics Society of IIT Delhi.

Prof. Vijay Kumar did his M.Sc. and Ph.D. in Solid State Physics at the University of Roorkee, India. He was a Humboldt Fellow and a scientist at Freie University Berlin, an Associate of the ICTP, Trieste, JSPS Invitation Fellow, Japan, a Senior Scientist at IGCAR, Kalpakkam and a Research Expert of IAEA & UNESCO at the ICTP where he directed many scientific activities. He was at Cavendish Laboratory, Cambridge and SISSA, Trieste as a Visiting Scientist and as a Visiting Professor at IMR, Tohoku University, Laboratoire Aime Cotton, CNRS, Orsay, Center for Interdisciplinary Research, Tohoku University, and the International Frontier Center for Advanced Materials (IFCAM) of IMR. He was the first Chairman of the subject group "Computer Aided Design of Materials" of the Materials Research Society of India (MRSI) and is a recipient of the MRSI Medal. He was President of the Indian Physics Association, Kalpakkam Chapter. Currently he is a Visiting Professor at the Laboratory for Advanced Materials of IMR and Founder President of the Dr Vijay Kumar Foundation, Chennai, India.

Yoshiyuki Kawazoe received his Dr. of Science from the Department of Physics, Tohoku University, in 1975, where he majored in theoretical nuclear physics. He was promoted to Full Professor in the Institute for Materials Research, Tohoku University, in 1990. In 1991 he received the Eastern Prize given by the Indian Embassy. Important publications include: "Phase Diagrams and Physical Properties of Nonequilibrium Alloys", Chief Editor, Springer-Verlag (1997), "Materials Design by Computer Simulation", Y. Kawazoe, K. Esfarjani and K. Ohno, Springer-Verlag (1999), and more than 50 books and more than 450 ISI journal papers.

Abhishek Kumar Singh

Vijay Kumar

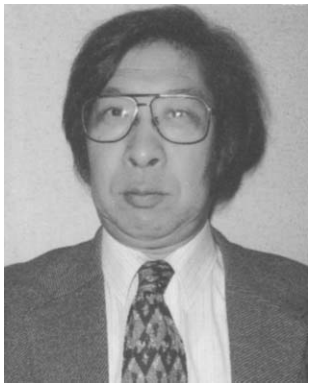

Yoshiyuki Kawazoe

DOI: 10.1039/b311850a

semiconducting depending upon their type, such as armchair or zigzag, the diameter and the chirality. They can be used as conductive wires,[2,3] to develop high strength composites,[4] energy storage and energy conversion devices,[5,6] flat panel displays[7] and radiation sources[8] as well as probes[9] (such as an STM and AFM tip) and chemical sensors.[10] Some of these applications are now being realized in products. A room temperature field-effect transistor of a semiconducting carbon nanotube has also been demonstrated.[11] It was fabricated by connecting two metal electrodes to a nanotube that was placed on a silicon substrate covered with a SiO_2 layer. The nanotubes were either randomly distributed or positioned on the substrate by atomic force microscopy.[12,13] The semiconducting nanotubes showed a gating effect while the metallic nanotubes showed a linear dependence of current–voltage curve with no dependence on the gate voltage. While these developments are exciting, there is the problem of separating semiconducting and metallic nanotubes. In a recent experiment[14] it has been shown that metallic and semiconducting nanotubes can be separated from the suspension using alternating current dielectrophoresis. However, conventional silicon based technology is so well established that only overwhelmingly compelling new technology will be able to replace it. Therefore, continuous efforts for the miniaturisation of silicon devices are worthy as these could prove more convenient and economical for commercialization than any other process. The fully grown up industry for device fabrication of silicon could prove vital in this respect, as any new development which does not involve silicon has to set up a whole new technology for the mass production of devices.

The most viable current alternative, carbon nanotubes, can be produced in small quantities at present but high quality impurity/defect free carbon nanotubes that one would need to produce in a controlled way for applications are still very uneconomical. There have been significant developments in recent years that show the importance of silicon even at the nanoscale. One such development is the single electron transistor (SET) memory made up of silicon.[15,16] SET is a field effect transistor that can be switched by a single electron operating under the standard conditions. It is similar to the conventional field-effect transistor except that the channel is a small ($\sim$10 nm) conducting island sandwiched between potential barriers. The barriers are high enough that the charge carriers can only reach the island through tunnelling. By applying a voltage at the nearby gate one can lower the barrier and the device becomes conducting. The SET operations are even being achieved at room temperature.[15] The most interesting thing is that the fabrication process relies only on the technology already developed for MOSFETs. Also even in the field of quantum computing, the importance of silicon has not been undermined. The proposed quantum computers[17] promise to exceed the computational efficiency of present day classical machines because of quantum algorithms that may require fewer steps to perform certain tasks. In such proposed computers the information is coded onto the nuclear spins of donor atoms in doped silicon electronic devices. Applications of Si nanowires (SiNWs) have also been explored. Boron doped silicon nanowires[18] have been shown to be highly sensitive and selective nanosensors for biological and chemical species. Amine and oxide functionalized SiNWs exhibit pH-dependent conductance that is linear over a large range of pH and could be understood in terms of the change in the surface charge during protonation and deprotonation. Biotin-modified SiNWs are used to detect streptavidin down to at least a picometer concentration range. Antigen functionalized SiNWs show reversible antibody binding and concentration dependent detection in real time.

An important aspect of silicon nanostructures is the possibility of luminescence in the visible range in contrast to the bulk that is a poor emitter of light due to its indirect band gap. In Si nanoparticles and SiNWs as the dimension reaches the carrier de Broglie wavelength, quantum confinement changes the gap energies leading to the possibility of visible photoluminescence[19] and novel devices in which electronics could be combined with photonics to create microphotonics using silicon. Currently III–V compounds are used for optical communication. However, there are problems of lattice mismatch and therefore, if silicon can be made in a form that gives photoluminescence, it can solve this problem. Recently light amplification has been demonstrated[20] from Si quantum dots dispersed in a SiO_2 matrix. These developments are promising and could lead to Si based lasers.

A recent significant development in nanostructures of silicon is the possibility to produce novel forms such as silicon fullerenes[21–27] and nanotubes[28–31] using metal encapsulation. These are more stable than nanostructures formed from elemental silicon, have high symmetries and potential for mass production with size selection. Their electrical, magnetic and optical properties can be changed by changing the metal atoms. Such metal encapsulated silicon clusters could be assembled to form new varieties of silicon. These developments are still in their infancy and could give way to components at the nanoscale for possible miniaturization of silicon-based devices. Many different properties such as metallic behaviour,[28] magnetism,[29] vibrational and optical properties[32] have already been found that are promising. The fullerene and the Frank–Kasper structures of $M@Si_{16}$ clusters have been predicted[21] to exhibit visible luminescence. Here we review some recent developments in nanoparticles and SiNWs and discuss the findings[28] of silicon nanotubes as well as their properties.

Computational approach

At the nanoscale the atomic structure of matter could be very different from the bulk and a quantitative understanding from experiments is also often difficult. Computer simulations can play a very important role in understanding the properties and phenomena under controlled conditions. It is also important that such calculations are performed using tools that have predictive capabilities. *Ab initio* electronic structure calculations based on the Kohn–Sham density functional theory (DFT) have been enormously successful using the local density approximation[33] (LDA) and more recently by taking into account the generalized gradient corrections[34] (GGA) that generally correct the over binding obtained by using the LDA, or by using the hybrid exchange-correlation functionals[35] that attempt to improve upon LDA/GGA. The advantage of the Kohn–Sham density functional approach is its simplicity as one needs to solve Hartree-like equations. Although different ways exist to solve the Kohn–Sham equations,[36] a plane wave basis approach using pseudopotentials[37] is quite efficient for understanding the chemical bonding and associated properties of such systems and seems to be most advantageous, particularly in cases where ion dynamics needs to be performed.[38] This basis set is complete and calculations can be performed for molecules, nanotubes, nanowires, quantum dots, perfect crystals, defects and surfaces of materials as different as semiconductors, simple and transition metals, insulators, *etc.* It provides a possibility to understand the evolution of the properties of matter from atomic and molecular levels to the bulk phase on an equal footing. In a large number of cases results obtained by this method often agree with experiments closely and even the predictions have received subsequent experimental support. Currently high accuracy calculations can be performed on systems having of the order of 1000 atoms while much larger systems can be treated with some approximate methods or by exploiting the symmetries in the system. This range is particularly exciting for

nanosystems having dimensions of a few nm. Such simulations can be very advantageous in exploring different possibilities even before experiments are done. Most of the results and predictions reported here have been obtained by using such approaches.

The results on metal doped silicon and germanium nanotubes and clusters as presented here are obtained using an *ab initio* ultrasoft pseudopotential plane wave method and GGA[34] for the exchange-correlation energy. We have studied clusters of silicon and germanium with metal doping and explored various structures in the pursuit of finding stable units with a particular number of Si and dopant atoms. The clusters are placed in a cubic box with periodic boundary conditions. The optimizations are performed using the conjugate gradient technique. The cut-off energy for the plane wave expansion depend on the TM atom, with a minimum of 227 eV for Mn and a maximum of 241 eV for Ni. Γ-point sampling is used for the Brilliouin zone integrations in the case of clusters and finite nanotubes. For infinite nanotubes a tetragonal cell is used and a few units of the clusters are considered in the cell in order to explore changes in the structure as well as magnetic ordering. Further 15 k-point sampling along the nanotube axis is used for the optimizations of the infinite nanotubes. Forces are converged to 0.001 eV $Å^{-1}$. Different initial guesses are used for the local magnetic moments, including ferromagnetic, antiferromagnetic, and non-magnetic spin configurations in order to find the lowest energy spin and atomic configurations of the nanotubes.

Nanoforms of elemental silicon: nanoparticles and nanowires

While clusters of silicon have been studied for quite some time, the finding of photoluminescence in porous silicon[39] led to much research on its nanoparticles.[19,40,41] The quantum confinement in nanoparticles changes the band gap and can give rise to luminescence in the visible range. Often such nanoparticles are covered with an oxide layer or the dangling bonds are terminated with hydrogen so that the inner structure of such nanoparticles is diamond type as in bulk silicon. Experimentally there are difficulties in preparing monodisperse nanoparticles and the characterization of defects and impurities at the silicon and oxide interface. SiNWs have also been made with diameters as small as about 10 nm using electron beam lithographic techniques.[42,43] This is an effort to stretch the limits of the silicon device fabrication to smaller and smaller dimensions. In a different approach known as the vapour-liquid-solid (VLS) approach,[44,45] metal clusters are used to produce SiNWs that have diameters of 20 to 100 nm,[46,47] which is still quite large.

Recently thinner SiNWs with high size selectivity and aspect ratios greater than 1000 have been produced in large quantities by using supersaturated clusters produced[48] by laser ablation as seeds. In this approach the diameters of the SiNWs can be controlled by appropriately selecting the size of the clusters by controlling the temperature, pressure and residence time. Vapours of metal and silicon atoms are created using laser ablation of a silicon–metal alloy (target material) such as $Si_{0.9}Fe_{0.1}$. The growth process of SiNWs from this vapour is believed to be as follows. Aggregation of atoms leads to metal–silicon cluster formation. These are kept in liquid form by choosing the temperature appropriately. Continuous evaporation of the target material leads to supersaturation of the liquid nanoparticles such that excess silicon atoms are expelled from the liquid cluster that prefers stoichiometric composition of Si_2Fe. This was determined from the analysis of the composition of the nanoparticles that were found to be invariably present on one end of nanowires. This observation is also suggestive of the VLS growth process. The excess silicon expelled from the nanoparticles grows in the form of a nanowire. The growth of the nanowire stops when the cluster solidifies. Defect free nanowires of silicon were grown with diameters ranging between 6 to 20 nm. These SiNWs were reported to be free from metal at least within 1 at%. The surface of these nanowires is coated with an amorphous oxide layer due to presence of oxygen in the chamber. This growth process received support from the fact that germanium nanowires were grown at about 400 K lower temperature. This is because the solidus line for Ge_2Fe lies about 400 K lower than the one for Si_2Fe. The germanium nanowires formed from this method had diameters from 3 to 9 nm. SiNWs were also formed by using Au clusters formed from the evaporation of 1 at% Au doped silicon target. As the solubility of Au is low, silicon is nearly completely removed from these clusters in the process of SiNW formation. This method can be applied to any material because a pulsed laser can be used to ablate the target that contains the desired metal catalyst component. By selecting the metal catalyst appropriately to form metal clusters, nanowires of almost any material can be synthesized. It makes this approach very much universally useful. This method produces very large quantities of nanowires. In a further related development monodisperse solution grown SiNWs[49] were produced using monodisperse alkanethiol-capped gold nanocrystals that direct the growth of nanowires. Generally these nanowires consist of a core of crystalline Si and oxide amorphous cladding. The thickness of this cladding can be varied to change the optical properties of nanowires. The absorption edge of these SiNWs is strongly blue shifted from the bulk 1.1 eV indirect band gap. These optical properties are mostly due to the quantum confinement apart from the possibility of contributions from the surface states. Another possibility to form nanowires without oxide layers is by termination of the dangling bonds by hydrogen.[50] These H-terminated SiNWs are even more oxidation-resistant than regular silicon wafer surfaces. SiNWs as thin as 1.3 nm can be formed. The energy gaps were found to increase with decreasing diameter from 1.1 eV for 7 nm to 3.5 eV for 1.3 nm.

Several theoretical efforts have also been made to understand the stability as well as the properties of SiNWs. Read *et al.*[51] performed *ab initio* pseudopotential calculations on H terminated (001) SiNWs with (110) surfaces. The band gap was calculated to be direct and at the zone centre. Thick whisker like wires of silicon have been studied in order to get the ground state of thinnest possible SiNWs[52] using molecular dynamics simulations with empirical potentials and the Wulff construction that relates the surface energy with the equilibrium shape. SiNWs with less than 6 nm diameters were found to have polycrystalline structures with five-fold symmetry rather than a single crystal type. The nanowires remain stable even at 1000 K in the molecular dynamics calculations. While results of such studies may change if *ab initio* calculations are done, these show that silicon nanostructures with such small dimensions are unstable and can be drastically different.

One of the routes to form nanostructures of silicon could be by cluster assembly in which stable clusters are assembled in one-, two-, or three-dimensions to form materials with novel properties. A few possibilities for such units have been explored. Also experimentally at least 100 nm long SiNWs of 3 to 7 nm diameter were prepared[53] by depositing silicon vapour onto highly oriented pyrolytic graphite. These nanowires were assembled parallel in bundles. Their structure was suggested to be an assembly of Si_{24} fullerene type clusters. While such fused structures could be stable, pure Si_n clusters with $n \leqslant 25$ prefer elongated structures[54–56] rather than empty cage fullerene structures. A transition to nearly spherical three-dimensional structures occurs at $n > 27$. The structural transition from elongated to compact structures is related to the onset of the formation of structures that can be considered

to be composed of irregular cages with a small number of silicon atoms inside.[56,57] These results also give a clear indication of the difficulty in forming very thin nanowires or nanotubes of silicon. A thin SiNW was studied using tricapped trigonal prism (TTP) Si_9 units and uncapped trigonal prisms[58] as the building blocks. Using full-potential linear muffin-tin orbital calculations such stacks of TTPs were found to be stable. They could be grown up to 26 Å along the nanowire axis. The binding energy (BE) and the gap reach towards saturation and zero value, respectively as the length of the wire is increased. The formation of thicker SiNWs has been studied from tight binding molecular dynamics calculations.[59] The stability of these SiNWs depends much upon the coordination of core atoms as they must be four-fold coordinated and must be surrounded by three-fold coordinated Si atoms. The outer surface of such SiNWs incorporates one of the most stable reconstructions at silicon surfaces. The building blocks for the SiNWs are multiply connected clusters with a small hollow region in the middle. Conductance of cluster assembled short SiNWs passivated by H and connected to aluminium electrodes has been studied[60] from DFT calculations. The short ($\sim$0.6 nm) nanowires were found to be fully metallized due to the metal-induced gap states while longer ($\sim$2.5 nm) nanowires form a nanoscale Schottky barrier with heights larger than the bulk value by 40 to 90%.

There have also been theoretical attempts reporting stabilization of silicon structures like carbon nanotubes. Fagan *et al.*[61] calculated the band structure of silicon nanotubes with the same armchair and zigzag atomic structures as carbon nanotubes and showed their electronic properties to depend on the chirality. They could be metallic or semiconducting similar to the carbon nanotubes. In another study using DFT the stability of tubular[62] forms of silicides such as $CaSi_2$ and SiH was explored. $CaSi_2$ has puckered layers of Si separated by Ca atoms that donate charge to Si. Therefore, the Si layer behaves like that of black phosphorous, which also has a puckered layered structure. Similarly a SiH layer has a graphene sheet like structure but it is puckered so that H atoms are on both the sides of the layer. Puckering in these layers gives a clear indication that sp^2 bonding is not favoured. However, their nanotube forms were studied by folding the puckered layers. The nanotubes formed in this way are semiconducting and it has also been shown that this does not depend upon the chirality of the nanotubes.

Metal encapsulated clusters: a new paradigm for making novel structures of silicon

Unlike carbon that can form sp, sp^2, and sp^3 bonded structures which provide the richness of carbon chemistry, silicon prefers sp^3 bonding and does not exist in sp^2 bonded form by itself and this is the reason that nanotube like structures of elemental silicon are not stable. An alternative approach in stabilizing the sp^2 bonding in silicon and also to form nanotubes could be by doping Si with metal atoms. The presence of metal atoms could facilitate sp^2 bonding in silicon as it has been found[63] in AlB_2 type compounds such as $Ca(Al_xSi_{1-x})_2$ or $Sr(Ga,Si)_2$ and could lead to the formation of nanotubes with metal atom encapsulation.[28] In these compounds there are large charge transfers between the Ca and Al/Si atoms and several possibilities of distributing Ca atoms have been tried.[64] However, a whole new series of developments have taken place recently in this field. The formation of metal encapsulated silicon and germanium clusters[19,21–27] has opened up new avenues to generate nanoforms of Si and Ge by assembly of such clusters with properties controlled by the metal atoms.[28–31]

The higher stability and symmetry as well as size selectivity of metal encapsulated clusters in contrast to those of pure Si or Ge offer the strong possibility of their large-scale production. One of the recent developments in this area is the finding of three high symmetry novel metal encapsulated cage clusters, which are fullerene like $M@Si_{16}$, cubic $M@Si_{14}$, and Frank–Kasper tetrahedral $M@Si_{16}$ clusters.[21] The size of the Si cage is found to depend strongly upon the size of the metal atom. The M–Si interactions are very strong and these lead to compact structures and control the size of the silicon cage. Doping of various metal atoms such as Zr, Ti, Hf, Cr, Mo, W, Ru, Os, Fe,... has been studied. One of the novel findings is the Frank–Kasper polyhedron of $Ti@Si_{16}$ that has an exceptionally large GGA gap of about 2.35 eV. Metal encapsulated clusters for Ge and Sn also show[23,24,65] novel properties similar to those of Si. In fact in some cases the band gaps of the lowest energy Ge based clusters[23] is even larger than the values for the ones based on silicon such as for $Zr@Ge_{16}$. The doping of Zn (Cd) in Ge_{12} (Sn_{12}) has also been shown[24] to lead to perfect icosahedral structure formation that has the lowest energy in both the cases. The highest symmetry as well as a large HOMO–LUMO gap of 2.12 eV (1.93 eV) for the metal-doped Ge (Sn) clusters make them behave like super atoms and attractive for self-assembly. Doping of Mn in such icosahedral cages also leads to clusters with large magnetic moments.[65] The weak cluster–cluster interactions,[21] metal like as well as covalent bonding, possibilities of varying band-gap with metal atom and the occurrence of magnetic moments in some cases, make these clusters novel for assembly. Such an assembly was explored to prepare quasi-one-dimensional structures of such metal encapsulated silicon clusters that led to the finding of silicon nanotubes, as discussed in the next section.

The finding of silicon nanotubes

As discussed in the previous section, nanotubes of elemental silicon are difficult to stabilize. The preference for sp^3 bonding in silicon and germanium leads to distortions in their quasi-one-dimensional tubular nanoforms so that they tend to become three-dimensional structures rather than to form nanotubes as shown in Fig. 1. Considering stacking of six-membered chair shape units of Si_6, the optimized structures of these short nanowires were found to show a tendency for agglomeration to 3-D structures. Several of the atoms become somewhat tetrahedrally coordinated. Therefore, the likelihood of long symmetric elemental Si wires of small dimensions is doubtful. This result is very much in agreement with previous studies done on silicon clusters that also found three-dimensional structures. M encapsulation leads to several new forms of silicon with differing properties and stabilizes cage type structures with a mixture of sp^2–sp^3 or even metallic like bonding. Therefore, the cluster assembly approach of such clusters could play an important role in developing novel nanostructures of Si.

Indeed it was shown[28] that the assembly of metal encapsulated clusters of Si leads to the stability of its nanotubes (Fig. 1). The strategy adopted to stabilize these finite nanotubes was quite simple. It was found[25] that a hexagonal prism structure of $Si_{12}W$ with W at the centre had the lowest energy. However, when such units were stacked to form a wire, these got distorted,[66] as the W atom is too big to continue such a stacking. Another study[24] explored the stability of various structures of $Si_{12}M$ with M a divalent metal atom. For M = Be the cluster was found to have a chair shaped structure with Be at the centre (see later). However, when two such $Si_{12}Be$ units were stacked,[28] surprisingly a transformation occurred from the chair-shaped units to the hexagonal shape as shown in Fig. 1. The Be atoms are displaced from the centre of the prism towards a ring. Taking three units of $Si_{12}Be$ the rings were again found to be stable and hexagonal in shape but the Be atoms were not symmetrically arranged and again displaced

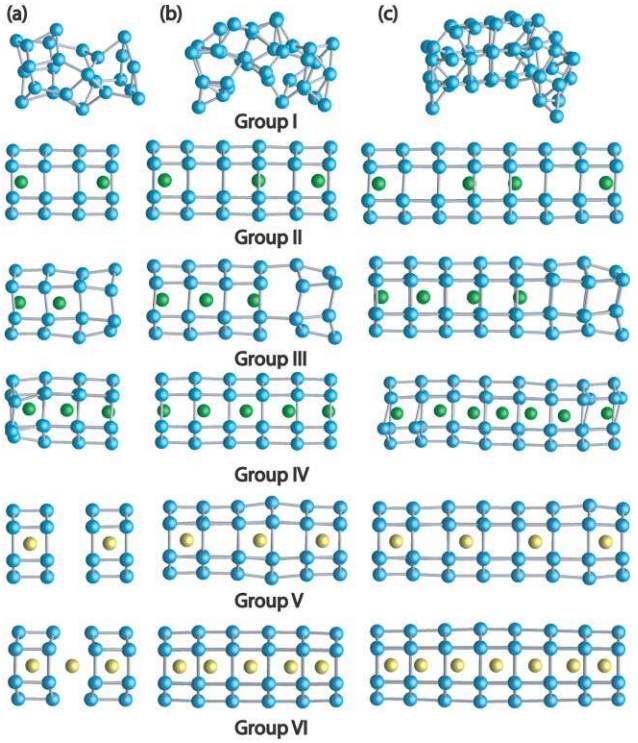

Fig. 1 Atomic structures of finite doped silicon nanotubes a, b, c, correspond to structures with 24, 36, and 48 Si atoms respectively. Group I shows deformation of nanotubes of elemental silicon formed by stacking of chair shaped Si_6 units. Group II shows almost perfect hexagonal rings obtained in finite Si_nBe_m (n, m = 24, 2; 36, 3; and 48, 4) nanotubes. Group III shows a different distribution of Be atoms for the same number of n and m as in Group II. Note that the undoped part of the nanotube tends to distort to chair shaped units. Group IV shows finite nanotubes of Si_nBe_m in which a Be atom is placed between all hexagonal prisms. They develop some distortions. Group V and VI show the same for Si_nMn_m. Note that in this case the structure becomes well ordered as seen for $Si_{48}Mn_7$. Similar features are also observed with other transition metal atoms such as Fe and Ni.

towards one of the hexagons in order to provide optimal bonding with the Si atoms. The third Be atom gets almost to the centre of the hexagonal ring. Studies on further doping and different arrangements of Be atoms showed that the doped portion of the nanotube was symmetric and nearly hexagonal in shape, while the undoped portion was distorted back to a chair shaped structure, giving a clear indication of the stabilization of sp^2 bonding due to metal atom doping. When Be atoms are placed between all the hexagonal rings, then some distortions occur in the nanotube structure as the size of the Be atom is small and it tries to optimize Be–Si and Si–Si interactions but basically the nanotube is stable.

It was noted that the packing of two units of $Si_{24}Be_2$ leads to a symmetric $(Si_{12}Be)_4$ nanotube (Fig. 1) with very small sp^3 character. Thus, $Si_{24}Be_2$ represents a stable unit that can be repeated to obtain a nanotube of desired length. The BEs for the different distributions of Be are rather similar. However, the highest occupied–lowest unoccupied molecular orbital (HOMO–LUMO) gap shows significant variation. It decreases as the length of the nanotube increases and finally the infinite nanotube becomes metallic. These results demonstrate that nanotubes with stoichiometry $(Si_{12}Be)_n$ are quite stable with hexagonal rings of silicon. Such rings have predominantly sp^2 bonding and therefore offer the possibility of new nanostructures of Si stabilized by the metal atoms.

Further study of the stability of doped infinite nanotubes with a unit cell of $Si_{12}Be$ and another unit cell of 24 Si atoms and two, three and four Be atoms showed them to be stable. These structures were optimized with respect to the cell size along the nanotube axis, allowing the atoms to relax freely. The

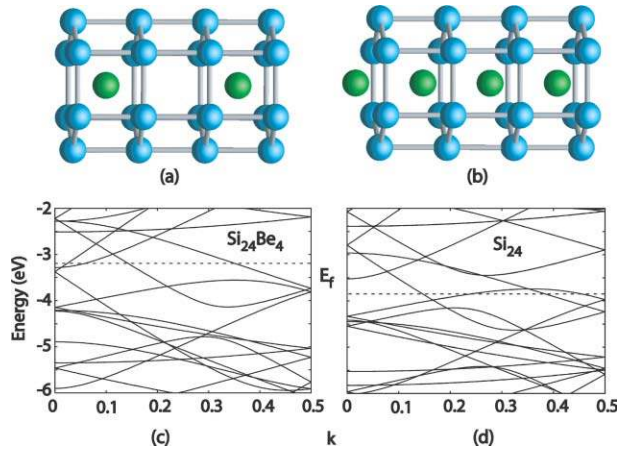

Fig. 2 Representative units used for infinite nanotubes of Si_nBe_m. (a) $Si_{24}Be_2$, (b) $Si_{24}Be_4$. These are metallic as can be seen from the band structure of $Si_{24}Be_4$ shown in (c). (d) Shows the band structure of Si_{24} infinite nanotube obtained by removing Be atoms in (b). This is also metallic.

BEs in these infinite nanotubes are higher than the values for the finite nanotubes. As in the finite nanotubes, it was found that the Be atoms in the lowest energy structures of $Si_{24}Be_2$, $Si_{24}Be_3$, and $Si_{24}Be_4$ infinite nanotubes were not exactly in between the hexagonal rings but slightly towards one ring (Fig. 2), though, for $Si_{12}Be$ cluster the Be atom is centred. The band structures of these nanotubes show metallic characteristics as shown in Fig. 2. This is not due to the doping of metal atoms. A calculation on the silicon nanotube without metal atoms also showed it to be metallic. Thus, in contrast to the carbon nanotubes for which metal doping generally does not change their structures, doping by metal atoms is very important for the stabilization of the Si nanotubes and in controlling the structure as shown here. The Si–Si bond lengths between the hexagonal rings as well as within a ring are similar and have covalent bonding. The density of states (see later) at the Fermi level for the infinite nanotubes is predominantly p type.

Magnetism in silicon nanotubes

The presence of metal atoms in silicon nanotubes also opens up the possibility of magnetism in these silicon-based structures.[29] For metal encapsulated silicon clusters, transition metals (TMs) have been shown[21–23,55] to be particularly important and these give rise to large embedding energies in the silicon cage and their stability. Therefore, it is likely that doping with TM atoms could also lead to the higher stability of the nanotubes. As the atomic size plays an important role, 3d TM elements seem to be most appropriate for doping, as the strain in the Si–Si bonds can be minimal due to smaller size mismatch. Following the case of Be doping, stability of a basic unit of $Si_{12}M$ was first explored that could be assembled to form nanotubes. As shown in Fig. 3 the hexagonal prism structure of $Si_{12}M$ was found to be lowest in energy for M = Mn, Fe, and Co as compared to the chair shape structure of $Si_{12}Be$ while in

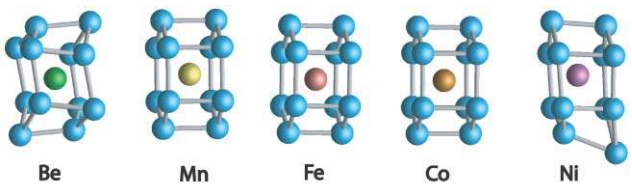

Fig. 3 Lowest energy structures with stoichiometry $Si_{12}M$ (M = Be, Mn, Fe, Co, and Ni).

the case of Ni, the structure is slightly distorted. The magnetic moment on these clusters have the values of 1, 0, 1, and 0 μ_B for M = Mn, Fe, Co, and Ni, respectively. Stacking two units of the hexagonal prism cluster leads to weak interaction between the units such as for $Si_{12}Mn$ and large separation between the units due to a large HOMO–LUMO gap (Fig. 1). Doping of one more metal atom in between the units leads to structures that are slightly curved in a symmetric manner (Fig. 1). However, continuation of assembling and doping of these units with one more TM atom in between the prisms leads to an increase in the BE of the nanotubes, an improved geometry with nearly planar Si hexagonal rings (Fig. 1) and generally an enhancement in the magnetic moments as shown for M = Fe in Fig. 4. The BE lies in the range of 3.88–4.25 eV atom^{-1} as compared to 3.62–3.86 eV atom^{-1} for Be doped nanotubes[28] as well as ordered hexagonal rings of Si.

The occurrence of magnetism in TM doped nanotubes is an interesting aspect for developing nanoforms of silicon. The magnetic moments of the TM atoms in the metal encapsulated silicon clusters are generally quenched due to the strong interaction with silicon atoms and hybridization between the TM atom d orbitals with the sp orbitals of Si. However, in finite Fe- and Mn-doped nanotubes, the local magnetic moments increase with an increase in the number of dopants for a given number of Si atoms (Fig. 4). Furthermore, for Fe doping there is a transition from antiferromagnetic to ferromagnetic coupling as the number of dopants is increased. The local moments of both Fe and Mn are highest towards the centre of the nanotubes and lowest at the ends. This is due to the fact that upon assembly of clusters, the charge on silicon atoms gets shared with the Si atoms in the neighbouring ring at the cost of the interaction with the metal atom. This helps to enhance the magnetic moments on the metal atoms away from the edges of the nanotube. The values of the local moments range from 1.0 to 2.6 μ_B for Fe and 0 to 3.6 μ_B for Mn. The magnetic moments of the Co-doped nanotubes are low, while the magnetic moments of the Ni-doped nanotubes are in most cases completely quenched. So as we go from Mn towards Ni, there is a general tendency of decreasing magnetic moments. This can in general be expected as the magnetic moments in TM atoms also show this trend.

When $Si_{12}M$ cluster units interact to form a nanotube, there is also an increase in the Si–Si and TM–Si bond lengths. This is also an indication for the weakening of the covalent bonding between the metal and the Si atoms. This can lead to the development of magnetic moments on the TM atoms particularly for elements with large atomic moments. A similar development of magnetic moments in the $Si_{12}Cr$ cluster was found when H atoms were attached on Si atoms.[66] Addition of H was found to lead to an increase in the size of the silicon hexagonal prism, which also gets distorted due to an enhancement in the sp^3 bonding. The Cr atom is displaced from the centre of the prism towards the centre of one of the hexagons. The H termination of these clusters has a somewhat similar effect as the linking of the clusters in the nanotubes. This is further supported from the fact that a small or zero local moment is found on the metal atoms towards the edges of the finite nanotubes while large moments occur on atoms that are away from the edges of the nanotubes. There is a systematic behaviour of the local magnetic moments as the TM atoms are changed. The moments decrease as we go from Mn to Ni. The TM atoms having larger atomic magnetic moments have higher local moments in the doped nanotubes while in the case of Ni, these remain quenched as its low atomic magnetic moments may be quenched by even a weaker hybridization. The high magnetic moments of $Si_{48}Fe_7$ (1.7 μ_B per Fe atom) and $Si_{48}Mn_7$ (1.6 μ_B per Mn atom) suggest that they could be useful for magnetic device applications.

The infinite nanotubes with the stoichiometry $Si_{24}M_4$ and $Si_{24}M_2$ also show enhanced stability as the number of M atoms is increased. An interesting finding has been the change in the position of the dopant atom. In the ferromagnetic phase of the infinite $Si_{12}M$ nanotube the M atom lies at 0.98, 0.79, and 0.27 Å away from a hexagonal ring for M = Mn, Fe, and Co, respectively. Ni lies at the centre of the hexagons as shown in Fig. 5. The BEs of all the infinite nanotubes are higher than the values for the corresponding finite nanotubes.

The infinite Fe-doped nanotube has ferromagnetic coupling with a high magnetic moment of 2.4 μ_B per Fe atom.[29] This value is nearly the same as in bulk Fe. The antiferromagnetically coupled Fe-doped nanotube is 0.70 eV higher in energy, indicating that the ferromagnetic phase is quite stable. The quasi-one-dimensionality of this nanotube along with its high moments makes it attractive for use as a nanoscale magnet. Mn

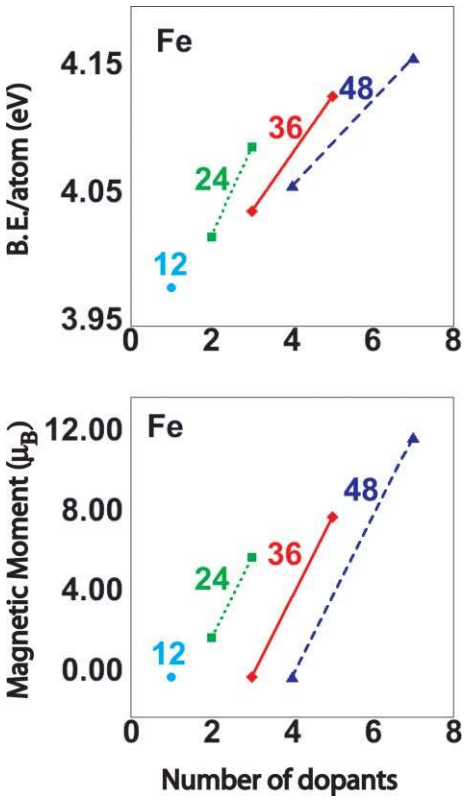

Fig. 4 Plots of BE atom^{-1} and magnetic moment per cell *vs.* the number of dopant atoms for the finite nanotubes of Si with Fe doping. The numbers on the curves show the number of Si atoms in the cell.

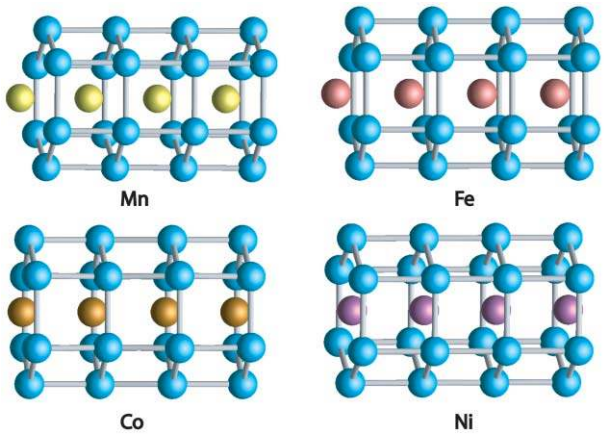

Fig. 5 Structures of $Si_{24}M_4$ (M = Mn, Fe, Co, and Ni) infinite nanotubes. Note the shift in the positions of metal atoms.

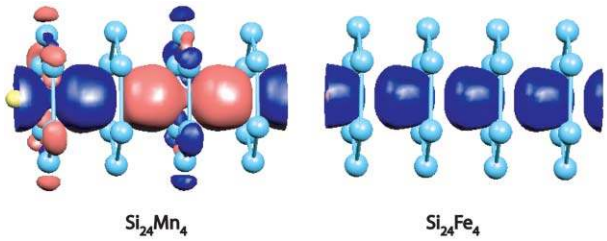

Fig. 6 Spin density of $Si_{24}Mn_4$ antiferromagnetically coupled and $Si_{24}Fe_4$ ferromagnetically coupled nanotubes. Blue/red isosurfaces show spin-up/down densities.

prefers an interesting spin arrangement in which pairs of ferromagnetically coupled Mn atoms are antiferromagnetically coupled with their neighbouring pairs (Fig. 6), resulting in zero net moment. The ferromagnetically coupled pairs are 2.55 Å apart as compared to 2.40 Å for the antiferromagnetically coupled pairs. Therefore, there is a dimerization of the antiferromagnetically coupled Mn atoms such that these are 1.12 and 1.18 Å away from the hexagons. The local magnetic moments on the Mn atoms range from 2.4 to 2.7 μ_B. This configuration, however, is only 0.03 eV lower in energy than the corresponding ferromagnetically coupled nanotube. This is another very important result as the transformation from antiferromagnetic to ferromagnetic coupling may be achieved by application of a weak magnetic field, suggesting that spin-polarized current flow could be controlled through application of a magnetic field. The charge densities for the antiferromagnetic $Si_{24}Mn_4$ and the $Si_{24}Fe_4$ nanotubes are shown in Fig. 5. It illustrates the localization of moments around the TM atoms. The BE for the Mn-doped nanotube is almost 90% of the bulk Si GGA cohesive energy. For the Co- and Ni-doped infinite nanotubes, ferromagnetic and antiferromagnetic starting configurations converge to non-magnetic solutions.

Fig. 7. shows the band structures of the Fe and Mn doped nanotubes. In all cases there is band crossing at the Fermi level for both the spin-up and spin-down components, indicating metallic behaviour. The band structure of the Mn-doped ferromagnetic nanotube shows a gap just above the Fermi energy for the spin-up component and therefore there could be interesting possibilities of making half-metallic nanotubes by inducing a small shift in the Fermi energy. The antiferromagnetic Mn-doped nanotube shows a quite different band structure, as the periodicities in the two cases are different. Fig. 8. shows the total and partial densities of states for $Si_{24}Mn_4$ infinite nanotube, which also reflects the large gap in the spin-up component. The majority of states for Mn lie well below the Fermi energy and the silicon 3p states contribute most to the states near the Fermi level.

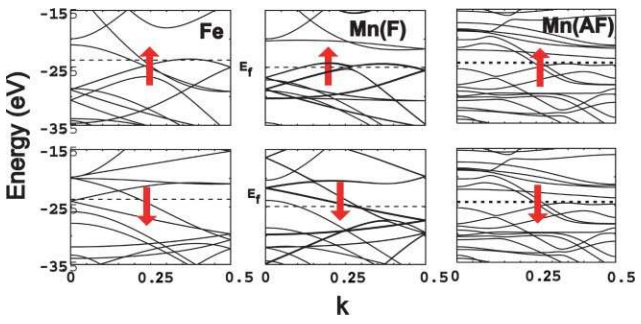

Fig. 7 Band structures of infinite nanotubes of ferromagnetic $Si_{24}Fe_4$, and ferromagnetic as well as antiferromagnetically coupled $Si_{24}Mn_4$.

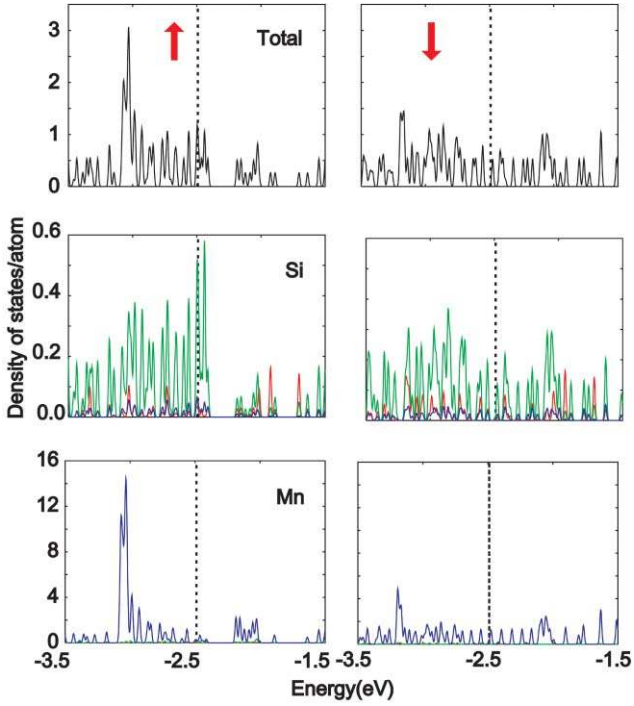

Fig. 8 Total and partial densities of states per atom of ferromagnetically coupled $Si_{24}Mn_4$ nanotubes. There is a significant gap for the spin-up component near the Fermi energy. Red, green, and blue represent s, p, and d components of the density of states on Si or Mn atoms.

Nanotubes of germanium

Recently it has also been shown that nanotubes of Ge[67] can also be formed by doping with metal atoms. However, in this case instead of hexagonal prism units, the lowest energy structure of $Ge_{12}M$ clusters is a hexagonal antiprism or an icosahedral structure. Both are nearly degenerate in the case of $Ge_{12}Mn$ clusters. The hexagonal antiprism has a magnetic moment of 1 μ_B while the icosahedral isomer has a large magnetic moment of 5 μ_B. The pentagonal and hexagonal units can be repeated to form finite or infinite pentagonal or hexagonal antiprism structures to develop nanotubes of Ge doped with Mn atoms as shown in Fig. 9. Both the pentagonal and hexagonal infinite nanotubes have the ferromagnetic state to be of the lowest energy. However, for the pentagonal antiprism nanotubes there is a transition to a ferrimagnetic state upon compression in which long-range ferromagnetic and short-range antiferromagnetic coupling become more favourable giving rise to nano-piezomagnetic behaviour in this tube. The hexagonal antiprism nanotube has the highest average magnetic moment, at 3.06 μ_B per Mn atom, found so far in metal doped nanotubes of semiconductors. These nanotubes are, therefore, interesting as nanomagnets, nanosensors and for other magnetic applications at the nanoscale.

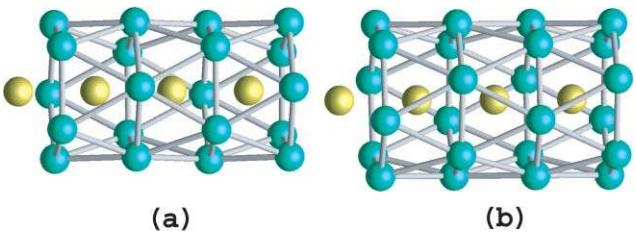

Fig. 9 Atomic structures of (a) $Ge_{20}Mn_4$ pentagonal and (b) $Ge_{24}Mn_4$ hexagonal antiprism nanotubes.

Effects of H and O adsorption

An understanding of the effects of adsorption of H or O is important for the study of the stability of the nanotubes. Also one would like to develop semiconducting nanotubes and interaction of H or O could provide a way in this direction. Furthermore, oxide layers are needed as the most fundamental component for the currently used MOSFET devices. The most important limiting factor for the present approach of device size miniaturisation is the thickness of the oxide layer. The work of Muller *et al.*[68] is an experimental proof of the fundamental limit to the size of the gate-oxide layer. Using an electron microscope in combination with spectroscopic analysis of the electron energy levels in the Si–SiO_2 interface, they showed that electronic wave functions penetrate through the ultra thin oxide layer from both ends. The electrical insulation area breaks down at less than 0.7 nm thickness of the oxide layer. In order to overcome this limitation at the nanoscale, we need perhaps an oxide layer thinner than the theoretical limit of the SiO_2 layer but possessing a higher dielectric constant. Unfortunately, all the material studied so far could not prove to be as good as SiO_2. At the nanoscale it may be possible that one could prepare a composition of silicon oxide that could have different properties. For this approach, oxidation of the nanotubes could be one possible way. There could also be possibilities of integrating device elements within the same nanotube by selective oxidation. Our initial calculations are encouraging and the nanotubes are stable upon oxygen interaction. A more deep and extensive study is underway and will be published separately.

Calculations on H interactions show that H leads to the development of sp^3 bonding and weakening of the M–Si interactions. Calculations on $Si_{24}Mn_4$ and $Si_{24}Fe_4$ infinite nanotubes show that the interaction with hydrogen leads to distortions in the nanotubes. So for thin nanotubes, H has the effect of breaking the nanotubes. However, somewhat thicker nanotubes with bulk sp^3 bonding could be possible as also suggested from experiments.[50]

Perspective/concluding remarks

We have reviewed briefly the recent developments in nanostructures of silicon and the findings of the silicon nanotubes in particular. It is shown that doping of a metal atom can stabilize the sp^2 bonded form of silicon that has metallic character. Doping of transition metal atoms leads to interesting magnetic behaviour that could lead to novel applications of such systems in the form of spin polarized transport in spintronics devices. These are the thinnest nanotubes and it would be natural to explore the stability of thicker nanotubes as from an experimental point of view, these are yet to be prepared and it could be possible that they occur in thicker forms. Further studies with adsorbents would be useful from the point of view of applications. Also in semiconductor technology, a semiconducting nanotube would be required. We are exploring the possibilities of making the same. Another interesting aspect of these nanotubes could be their conducting properties. Suitable doping could modify the conduction properties in these nanotubes. This could lead to interesting conduction behaviour in that the conduction in such nanotubes could be predominantly along the metal atom chain or the Si tube or both. Metal encapsulation has opened up a new paradigm in silicon nanostructures, as one may be able to prepare metallic, magnetic, semiconducting nanotubes for diverse applications in devices. We hope experimental studies will be undertaken to explore their formation.

Acknowledgements

The authors would like to thank the staff of the Centre for Computational Materials Science at the Institute for Materials Research, Tohoku University for the use of the Hitachi SR8000/64 supercomputing facilities. A. K. S. is grateful for the support of MEXT fellowship. V. K. is thankful for the hospitality at the Institute for Materials Research and the support of JSPS.

References

1 S. Iijima, *Nature*, 1991, **354**, 56.
2 W. Liang, M. Bockrath, D. Bozovic, J. H. Hafner, M. Tinkham and H. Park, *Nature*, 2001, **411**, 665.
3 S. P. Franh, P. Poncharal, Z. L. Wang and W. A. de Heer, *Science*, 1998, **280**, 1744.
4 M. J. Biercuk, M. C. Llaguno, M. Radosavljevic, J. K. Hyun, A. T. Johnson and J. E. Fischer, *Appl. Phys. Lett.*, 2002, **80**, 2767.
5 Y. Chen, D. T. Shaw, X. D. Bai, E. G. Wang, C. Lund, W. M. Lu and D. D. L. Chung, *Appl. Phys. Lett.*, 2001, **78**, 2128.
6 A. C. Dillon and M. J. Heben, *Appl. Phys. A.*, 2001, **72**, 133.
7 N. S. Lee, D. S. Chung, I. T. Han, J. H. Kang, Y. S. Choi, H. Y. Kim, S. H. Park, Y. W. Jin, W. K. Yi, M. J. Yun, J. E. Jung, C. J. Lee, J. H. You, S. H. Jo, C. G. Lee and J. M. Kim, *Diamond Relat. Mater.*, 2001, **10**, 265.
8 H. Sugie, M. Tanemura, V. Filip, K. Iwata, K. Takahashi and F. Okuyama, *Appl. Phys. Lett.*, 2001, **78**, 2578.
9 C. L. Cheung, J. H. Hafner, T. W. Odom, K. Kim and C. M. Lieber, *Appl. Phys. Lett.*, 2000, **76**, 3136.
10 P. G. Collins, K. Bradley, M. Ishigami and A. Zettel, *Science*, 2000, **287**, 1801.
11 S. J. Tans, A. R. M. Verschueren and C. Dekker, *Nature*, 1998, **393**, 49.
12 S. Martel, T. Schmidt, H. R. Shea, T. Hartel and Ph. Avouris, *Appl. Phys. Lett.*, 1998, **73**, 2447.
13 A. Bachtold, P. Headly, T. Nakenishi and C. Dekker, *Science*, 2001, **294**, 1317.
14 R. Krupke, F. Hennrich and H.v. Lohneysen. M. M. Kappes, *Science*, 2003, **301**, 344.
15 L. Guo, E. Leobandung and S. Chou, *Science*, 1997, **275**, 649.
16 S. Tiwari, F. Rana, H. Hanafi, A. Hartstein, E. F. Crabbe and K. Chan, *Appl. Phys. Lett.*, 1996, **68**, 1377.
17 B. E. Kane, *Nature*, 1998, **393**, 133.
18 Y. Cui, Q. Wei, H. Park and C. M. Lieber, *Science*, 2001, **293**, 1289.
19 L. Brus, *J. Phys. Chem.*, 1994, **98**, 3575.
20 L. Pavesi, L. D. Negro, C. Mazzoleni, G. Franzò and F. Priolo, *Nature*, 2000, **408**, 440.
21 V. Kumar and Y. Kawazoe, *Phys. Rev. Lett.*, 2001, **87**, 45503.
22 V. Kumar and Y. Kawazoe, *Phys. Rev. B*, 2002, **65**, 73404.
23 V. Kumar and Y. Kawazoe, *Phys. Rev. Lett.*, 2002, **88**, 235540.
24 V. Kumar and Y. Kawazoe, *Appl. Phys. Lett.*, 2002, **86**, 859.
25 H. Hiura, T. Miyazaki and T. Kanayama, *Phys. Rev. Lett.*, 2001, **86**, 1733.
26 V. Kumar, C. Majumder and Y. Kawazoe, *Chem. Phys. Lett.*, 2002, **363**, 319.
27 V. Kumar, *Eur. Phys. J. D*, 2003, **24**, 227.
28 A. K. Singh, V. Kumar, T. M. Briere and Y. Kawazoe, *Nano Lett.*, 2002, **2**, 1243.
29 A. K. Singh, T. M. Briere, V. Kumar and Y. Kawazoe, *Phys. Rev. Lett.*, 2003, 91.
30 M. Menon, A. N. Andriotis and G. E. Froudakis, *Nano Lett.*, 2002, **2**, 301.
31 A. N. Andriotis, G. Mpourmpakis, G. E. Froudakis and M. Menon, *New J. Phys.*, 2002, **4**, 78.
32 V. Kumar, T. M. Briere and Y. Kawazoe, *Phys. Rev. B*, 2003, 68.
33 W. Kohn and L. Sham, *Phys. Rev. A*, 1965, **140**, A1133.
34 J. P. Perdew, in *Electronic Structure of Solids'91*, 1991, eds. P. Ziesche and H. Eschrig, Akademie Verlag, Berlin; J. P. Perdew, S. Kurth, A. Zupan and P. Blaha, *Phys. Rev. Lett.*, 1999, **82**, 2544; J. F. Dobson and J. Wang, *Phys. Rev. B*, 2000, **62**, 10038.
35 A. D. Becke, *J. Chem. Phys.*, 1993, **98**, 5648; A. D. Becke, *J. Chem. Phys.*, 1998, **109**, 2092.
36 V. Kumar, O. K. Andersen and A. Mookerjee, eds., *Methods of Electronic Structure Calculations*, 1994, World Scientific, Singapore.
37 G. Kresse and J. Furthmuller, *Phys. Rev. B*, 1996, **54**, 11169; *Comput. Mater. Sci.*, 1996, **6**, 15.

38 R. Car and M. Parrinello, *Phys. Rev. Lett.*, 1985, **55**, 2471.
39 L. T. Canham, *Appl. Phys. Lett.*, 1990, **57**, 1046.
40 S. Schuppler, S. L. Friedman, M. A. Marcus, D. L. Adler, Y.-H. Xie, F. M. Ross, T. D. Harris, W. L. Brown, Y. J. Chabal, L. E. Brus and P. H. Citrin, *Phys. Rev. Lett.*, 1994, **72**, 2648.
41 M. V. Wolkin, J. Jorne and P. M. Fauchet, *Phys. Rev. Lett.*, 1999, **82**, 197; J. P. Wilcoxon, G. A. Samara and P. N. Provencio, *Phys. Rev. B*, 1999, **60**, 2704.
42 T. Tsutsumi, K. Ishii, H. Hiroshima, S. Hazra, M. Yamanaka, I. Sakata, H. Taguchi, E. Suzuki and K. Tomizawa, *J. Vac. Sci. Technol., B*, 2000, **18**, 2640.
43 T. Ito and S. Okazaki, *Nature*, 2000, **406**, 1027.
44 R. S. Wagner and W. C. Ellis, *Appl. Phys. Lett.*, 1964, **4**, 89.
45 R. S. Wagner, in *Whisker Technology*, A. P. Levitt, ed., Wiley Interscience, New York, 1970, p. 44.
46 M. Yazawa, M. Koguchi, A. Muto, M. Ozawa and K. Hiruma, *Appl. Phys. Lett.*, 1992, **61**, 2051.
47 J. Westwater, D. P. Gosain, S. Tomiya, S. Usui and H. Ruda, *J. Vac. Sci. Technol., B*, 1997, **15**, 554.
48 A. M. Morales and C. M. Lieber, *Science*, 1998, **279**, 208.
49 J. D. Holmes, K. P. Johnston, R. C. Doty and B. A. Korgel, *Science*, 2000, **287**, 1471.
50 D. D. D. Ma, C. S. Lee, F. C. K. Au, S. Y. Tong and S. T. Lee, *Science*, 2003, **299**, 1874.
51 A. J. Read, R. J. Needs, K. J. Nash, L. T. Canham, P. D. J. Calcott and A. Qteish, *Phys. Rev. Lett.*, 1992, **69**, 1232.
52 Y. Zhao and B. I. Yakobson, *Phys. Rev. Lett.*, 2003, **91**, 35501.
53 B. Marsn and K. Sattler, *Phys. Rev. B*, 1999, **60**, 11593.
54 K. Ho, A. A. Shvartsburg, B. Pan, Z. Lu, C. Wang, J. G. Wacker, J. L. Fye and M. F. Jarrold, *Nature*, 1998, **392**, 582.
55 Q. Sun, Q. Wang, T. M. Briere, V. Kumar, P. Jena and Y. Kawazoe, *Phys. Rev. B*, 2002, **65**, 235417.
56 L. Mitas, J. C. Grossman, I. Stich and J. Tobik, *Phys. Rev. Lett.*, 2000, **84**, 1479.
57 U. Rothlisberger, W. Andreoni and M. Parrinello, *Phys. Rev. Lett.*, 1994, **72**, 665.
58 B. Li, P. Cao, R. Q. Zeng and S. T. Lee, *Phys. Rev. B*, 2002, **65**, 125305.
59 M. Menon and E. Richter, *Phys. Rev. Lett.*, 1999, **83**, 792.
60 U. Landman, R. N. Barnett, A. G. Scherbakov and Ph. Avouris, *Phys. Rev. Lett.*, 2000, **85**, 1958.
61 S. B. Fagan, R. J. Baierle, R. Mota, A. J. R. da Silva and A. Fajio, *Phys. Rev. B*, 1999, **61**, 9994.
62 G. Seifert, H. M. Urbassek, E. Harnandez and T. Frauenheim, *Phys. Rev. B*, 2001, **63**, 193409.
63 M. Imai, K. Nishida, T. Kimura and H. Abe, *Appl. Phys. Lett.*, 2002, **80**, 1019.
64 S. Gemming and G. Seifert, *Phys. Rev. B*, 2003, **68**, 75416.
65 V. Kumar and Y. Kawazoe, *Appl. Phys. Lett., 2003.*
66 V. Kumar and Y. Kawazoe, *Phys. Rev. Lett.*, 2003, **90**, 55502.
67 A. K. Singh, V. Kumar and Y. Kawazoe, submitted for publication.
68 D. A. Muller, T. Sorsch, S. Moccio, F. H. Baumann, K. Evans-Lutterodt and G. Timp, *Nature*, 1999, **399**, 758.